Chapter 6

Diffusion-at-a-constant-speed of photons: The 'strong' constraint of constant speed

6.1 Introduction

In the previous Chapter-5, we examined some models of photon migration, where, though the speed of the particle was not kept fixed locally, there was a global constraint on the particle in some average sense, i.e., the 'weak' constraint. In this Chapter, we will develop a model for photon migration, where we will implement the 'strong' constraint of fixed speed of the photon. It should be noted that this fixed speed would correspond to the group velocity of the photon wave packet. In this description, we will neglect the dispersive effects of the underlying structure of the medium on the wave. In the approximate description of light as a particle undergoing random scattering events, the speed in between the scattering events should be kept constant at the very least. There is only a change in the direction of propagation at each scattering event. We accomplish this by taking a clue from the simplest case of accelerated motion involving no change in the kinetic energy, i.e., motion along a circle where the forces act only perpendicular to the velocity of the particle. We can imagine that the photon during its random walk is instantaneously moving along a circle, whose radius is a random function of time. It must be remarked here again that the wave nature and polarization effects are ignored and light is treated as a particle in a medium which exerts *transverse* fluctuating forces on the particle, *i.e.*, the force is perpendicular to the instantaneous velocity vector. Also, as before, while the actual disorder is maybe in space (quenched disorder), all current treatments in-

cluding ours, are in terms of a Brownian motion (temporal disorder *i.e.*, a stochastic process).

Essentially, we describe the light propagation in a stochastic medium as the motion of a kind of Brownian particle on which the fluctuating forces act only perpendicular to the direction of its velocity. This is effective in strictly and dynamically preserving the speed of the particle. We call this the 'modified Ornstein-Uhlenbeck process'. This process is shown to correspond to a diffusion in the angular co-ordinate in the velocity space for a white-noise disorder. Exact expressions for the moments of the space variables are presented and the second cumulant approximation is shown to yield a Gaussian expression similiar to the traditional Ornstein-Uhlenbeck theory of Brownian motion. An expression is derived for the probability distribution for the large random force strength which preserves the light cone. The exact Fokker-Planck equation for the probability distribution is derived from the stochastic Langevin equations for the white-noise process. Numerical solutions of this equation are presented . It is shown that the probability distribution in infinite media is strongly forward peaked for short times and randomizes only at times of about $8t^*$ to $10t^*$. We have also solved numerically the equation for a semi-infinite geometry and obtained the persistence exponent of 0.435 ± 0.005 in two dimensions for this process. Solutions for a finite geometry are also given, showing that the effective diffusion coefficient as measured in a pulse transmission experiment through very thin slabs ($L \sim l^*$) would be lowered. We will also present results for the point spread function of a point source for transmission through a disordered slab. Finally we will discuss the case of an amplifying random medium.

6.2 The modified Ornstein-Uhlenbeck process

Light scattering in a stochastic medium is treated as a probabilistic process where each scattering event only changes the direction of the photon. The equation for the motion of a randomly accelerated particle with the special condition that the random forces always act only perpendicular to the velocity can be written as

$$\ddot{\vec{r}} \times \dot{\vec{r}} \times fit). \tag{6.1}$$

This we term as the modified Ornstein-Uhlenbeck process.

We will consider two dimensions for simplicity, and write for the motion in the xy-plane,

$$\ddot{x} = -f(t)\dot{y}, \tag{6.2}$$

$$\ddot{y} = f(t)\dot{x}, \tag{6.3}$$

where the force term $f(t)$ is a random function of time. We will assume a delta-correlated random force with Gaussian distribution. *i.*e.,

$$\langle f(t)\rangle = 0, \tag{6.4}$$

$$\langle f(t)f(t')\rangle = \Gamma\delta(t-t'), \tag{6.5}$$

and all higher cumulants of $f(t)$ being zero. This makes our treatment most valid for a very dense collection of highly forward scattering weak anisotropic scatterers. This set of stochastic Langevin equations yields on integration a first constant of integration $x^2 + \dot{y}^2 = c^2$, where c is the constant speed. So we can choose $x = c\cos\theta(t)$ and $\dot{y} = c\sin\theta(t)$ where $\theta(t)$ is some function of t. θ is recognized to be the angular co-ordinate in the velocity space. Substituting these expressions back into equation(6.2,6.3), we obtain $\dot{\theta} = f(t)$ or

$$\theta(t) - \theta_0 = \int_0^t f(t)dt\ . \tag{6.6}$$

Hence $\theta(t)$ follows a Wiener process and we can write the probability for $\theta(t)$ as

$$P_t(\theta) = \left(\frac{1}{2\pi\Gamma t}\right)^{\frac{1}{2}} \exp\left\{-\frac{(\theta-\theta_0)^2}{2\Gamma t}\right\}. \tag{6.7}$$

This is the result for a diffusion in 8, the angular co-ordinate in the velocity space, and we recognize this modified O-U process to be a random walk on the circle of radius c in the velocity space. Constraining θ to the range $[0, 2\pi]$, *i.e.*, identifying 8 with $\theta + 2n\pi$ for n an integer, we get the marginal probability distribution for 0.

$$P_t(\theta) = \sum_{n=-\infty}^{\infty} \left(\frac{1}{2\pi\Gamma t}\right)^{\frac{1}{2}} \exp\left\{-\frac{(\theta-\theta_0+2n\pi)^2}{2\Gamma t}\right\} \tag{6.8}$$

The value of θ_0 can be conveniently chosen to be zero.

Similiarly, in three dimensions, we have $\vec{f}(t) = [f_x(t), f_y(t), f_z(t)]$, where $f_x(t)$, $f_y(t)$ and $f_z(t)$ are uncorrelated random functions of time, and are assumed to be white-noise:

$$\langle f_i(t)\rangle = 0, \quad \langle f_i(t)f_j(t)\rangle = \Gamma\delta(t-t')\delta_{ij}. \tag{6.9}$$

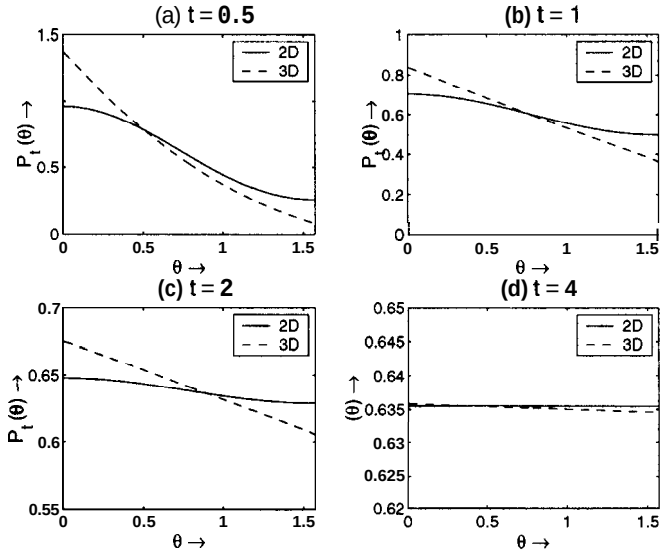

Figure 6.1: The marginal probability distributions for the angular co-ordinate in two dimensions (solid line) and three dimensions (dotted lines)

As before, integration of the above stochastic Langevin equation yields a first constant of integration as $x^2 + y^2 + \dot{z}^2 = c^2$. Proceeding as before, we reach the conclusion that again we have a diffusion for the angular coordinate in the velocity space. In three dimensions, we have a diffusion on the velocity sphere of radius c. The result for diffusion on the surface of a sphere is well-known and the marginal probability distribution for $\theta(t)$ and $\phi(t)$ (the polar angles) is given by:

$$P_t(\theta,\phi) = \frac{1}{2\pi}\sum_{l=0}^{\infty}\frac{2l+1}{4\pi}\exp\left[-\frac{l(l+1)t}{c^2}\right]P_l(\cos\theta), \tag{6.10}$$

where the z-axis is chosen along the initial direction ($\theta_0 = 0$). This results in a uniform distribution for ϕ. We show a plot of the probability distributions for 8 in two and three dimensions in Fig. 6.1.

Now we will derive the probability distribution function in the phase space. Consider the system of stochastic Langevin equations (again in 2-D for simplicity),

$$\dot{x} = u, \tag{6.11}$$

$$\dot{y} = v, \tag{6.12}$$

$$\dot{u} = -f(t)v, \tag{6.13}$$

$$\dot{v} = f(t)u. \tag{6.14}$$

Let $\Pi(x, y, \mathrm{u}, \mathrm{v})$ be the phase space density of points for the given system and U be the vector (x, y, u, v). Now, Π satisfies the stochastic Liouville equation.

$$\frac{\partial n}{\partial t} + \nabla_{\mathbf{U}} \cdot (\mathrm{un}) = 0, \tag{6.15}$$

where $\nabla_{\mathbf{U}} = (\frac{\partial}{\partial x}, \frac{\partial}{\partial y}, \frac{\partial}{\partial u}, \frac{\partial}{\partial v})$. Substituting for U and averaging over all possible configurations of disorder, by the van Kampen Lemma [98], the probability distribution $P(x, \mathrm{y}, u, \mathrm{v}) = \langle \Pi(x, \mathrm{y}, \mathrm{u}, \mathrm{v}) \rangle$ and satisfies,

$$\frac{\partial P}{\partial t} + u\frac{\partial P}{\partial x} + v\frac{\partial P}{\partial y} - v\frac{\partial}{\partial u}\langle f(t)\Pi \rangle + u\frac{\partial}{\partial v}\langle f(t)\Pi \rangle = 0 \tag{6.16}$$

By the Novikov theorem [100] (see Appendix B) for a white-noise process $\mathrm{f}(t)$,

$$\begin{aligned} \langle f(t)\Pi[f(t)] \rangle &= \frac{\Gamma}{2}\langle \frac{\delta\Pi[f]}{\delta f(t)} \rangle, \\ &= \frac{\Gamma}{2}\left(v\frac{\partial P}{\partial u} - u\frac{\partial P}{\partial v} \right). \end{aligned} \tag{6.17}$$

Using the above, we obtain for P(x,y,u,v) the differential equation

$$\frac{\partial P}{\partial t} + u\frac{\partial P}{\partial x} + v\frac{\partial P}{\partial y} = \frac{\Gamma}{2}\left(u\frac{\partial}{\partial v} - v\frac{\partial}{\partial u} \right)^2 P. \tag{6.18}$$

Now expressing u and v in terms of the angular co-ordinate 8, we finally get

$$\frac{\partial P}{\partial t} + c\ \cos\theta\frac{\partial P}{\partial x} + c\ \sin\theta\frac{\partial P}{\partial y} = \frac{\Gamma}{2}\frac{\partial^2 P}{\partial \theta^2}. \tag{6.19}$$

This can be generalized to three dimensions as

$$\frac{\partial P}{\partial t} + \vec{v} \cdot \vec{\nabla}_r P = \frac{\Gamma}{2}\nabla^2 P, \tag{6.20}$$

where $\vec{\nabla}_r = (\partial/\partial x, \partial/\partial y, \partial/\partial z)$, $\vec{v} = (\dot{x}, \dot{y}, \dot{z})$ and ∇_s^2 is the angular Laplacian given

$$\nabla_s^2 = \frac{1}{\sin\theta}\frac{\partial}{\partial\theta}(\sin\theta\frac{\partial P}{\partial\theta}) + \frac{1}{\sin^2\theta}\frac{\partial^2 P}{\partial\phi^2}, \tag{6.21}$$

in polar-spherical co-ordinates. This differential equation explicitly preserves the constancy of the speed of the photon. This Fokker-Planck equation is the same equation which was intuitively written down in Ref.[152, 153, 154]. It is rigorously proved therein that this has a path integral solution and the two approaches are equivalent. It appears that this equation in two dimensions has solutions in terms of

the Mathieu functions. This is easily seen by taking a Laplace-Fourier transformation with respect to the time-space giving:

$$\frac{d^2\tilde{P}}{d\theta^2} + (-s - k\cos\theta)\tilde{P} = -\delta(\theta - \theta_0)\delta(x - x_0) \tag{6.22}$$

which is a Mathieu equation for $\tilde{P}(\theta; s, \mathrm{k}) = \int_0^\infty \mathrm{dt}\ e^{-st} \int_{-\infty}^{+\infty} e^{ikx} P(x, 0; \mathrm{t})\ \mathrm{dx}\ d\theta$ (here y-invariance has been assumed). Similiarly, the Equation(6.20) seems to have solutions in terms of Legendre polynomials. However, we have not been able to explicitly solve the equations analytically.

6.3 Solutions in unbounded media

In this Section, we will investigate the nature of the solutions of this modified Ornstein-Uhlenbeck process for a particle moving in an unbounded medium. The relevant boundary condition is then that the probability vanishes for $|r| >$ ct in space.

6.3.1 Moments of the displacement and the cumulant expansion

The moments of the displacement can, however, be calculated analytically. The displacement can be written in terms of 0 as (in 2-D)

$$x - x_0 = \int_0^t c\ \cos\theta d\theta, \tag{6.23}$$

$$\mathrm{y} - y_0 = \int_0^t \mathrm{c}\ \sin\theta d\theta. \tag{6.24}$$

Using these and a Gaussian distribution for f (t), we get

$$\langle \mathrm{x} - x_0 \rangle = \frac{2c}{\Gamma}\cos\theta_0 \left(1 - e^{-\frac{\Gamma t}{2}}\right), \tag{6.25}$$

$$\langle y - y_0 \rangle = \frac{2\mathrm{c}}{\Gamma}\sin\theta_0\ (1 - e^{-\frac{\Gamma t}{2}}), \tag{6.26}$$

$$\langle (x - x_0)^2 \rangle = c^2 \left[\frac{2t}{\Gamma} - \frac{2}{3}\left(\frac{2}{\Gamma}\right)^2 \left(1 - e^{-\frac{\Gamma t}{2}}\right) - \frac{1}{12}\left(\frac{2}{\Gamma}\right)^2 \left(1 - e^{-\Gamma t}\right)\right], \tag{6.27}$$

$$\langle (\mathrm{y} - y_0)^2 \rangle = c^2 \left[\frac{2t}{\Gamma} - \frac{4}{3}\left(\frac{2}{\Gamma}\right)^2 (\mathrm{I} - e^{-\frac{\Gamma t}{2}}) + \frac{1}{12}\left(\frac{2}{\Gamma}\right)^2 \left(1 - e^{-\Gamma t}\right)\right], \tag{6.28}$$

$$\langle (x - x_0)(y - \mathrm{yo}) \rangle = 0. \tag{6.29}$$

This reproduces the result of the traditional Ornstein-Uhlenbeck process in that the first moment saturates at a mean free path l^* and the second moment increases

linearly with time at long times ($\Gamma t/2 \gg 1$). For short times ($\Gamma t/2 \ll 1$), however, the longitudinal spread (Ax^2) $\sim$ t^2 and the lateral spread (Ay^2) $\sim$ t^3, which are considerably slower than the diffusive linear behaviour. From these relations, we identify the mean free time t* to be $2/\Gamma$ and the transport mean free path $l^* = ct^*$. The diffusion coefficient is identified as the coefficient of the linear term of the second moment *i.e.*, c^2/Γ.

It is of interest to note that analytic expressions for the moments of all orders for the displacement can be obtained. The n^{th} order moment is given by

$$\langle (x - x_0)^n \rangle = c^n \int_0^t \int_0^t \cdots \int_0^t dt_n dt_{n-1} \cdots dt_1 (\cos\theta(t_1)\ \cos\theta(t_2) \cdot \cdot \cos\theta(t_n)\rangle. \quad (6.30)$$

Writing $\theta(t_i)$ as θ_i, the quantity within the angular brackets can be expressed as follows,

$$\begin{aligned} \langle \cos\theta_1\ \cos\theta_2 \cdots \cos\theta_n \rangle &= 2^{-n} \langle\ (e^{i\theta_1} + e^{-i\theta_1})(e^{i\theta_2} + e^{-i\theta_2}) \cdots (e^{i\theta_n} + e^{-i\theta_n})\ \rangle, \\ &= 2^{-n} \sum_{\substack{\sigma_1,\sigma_2\cdots\sigma_n \\ \sigma_i = \pm 1}} \langle\ \exp[i \sum_{j=1}^{n} \sigma_j \theta_j]\ \rangle. \end{aligned} \quad (6.31)$$

This can be expressed as a path integral using a Gaussian distribution for $f(t)$.

$$\begin{aligned} \langle\ \exp[i \sum_{j=1}^{n} \sigma_j \theta_j]\ \rangle &= \int \mathcal{D}[f(t)] \exp\left\{ - \int_0^t \left[\frac{f^2(t')}{2\Gamma} + i \sum_{j=1}^{n} \sigma_j f(t') \right] dt' \right\}, \\ &= \exp\left\{ -\frac{\Gamma}{2} \sum_{k=1}^{n} \left(\sum_{j=k}^{n} \sigma_j \right)^2 (t_k - t_{k-1}) \right\}, \end{aligned} \quad (6.32)$$

where $t_0 = 0$ and we assumed a time ordering of $t_1 < t_2 < \ \cdots\ < t_n$. Thus,

$$\begin{aligned} \langle (x - x_0)^n \rangle = c^n (n!) 2^{-n} \int_0^t dt_n \int_0^{t_n} dt_{n-1} \cdot \cdot \int_0^{t_2} dt_1 \times \\ \times \sum_{\substack{\sigma_1,\sigma_2\cdots\sigma_n \\ \sigma_i = \pm 1}} \exp\left\{ -\frac{\Gamma}{2} \sum_{k=1}^{n} \left(\sum_{j=k}^{n} \sigma_j \right)^2 (t_k - t_{k-1}) \right\} \end{aligned} \quad (6.33)$$

A similiar expression can be obtained for the $\langle (y - y_0)^n \rangle$ by noting that $\sin\theta = \cos(\pi/2 - \theta)$.

Now we can obtain the joint probability distribution of x and y as

$$P(x, y, t; x_0, y_0, 0) = \langle\ \delta(x - x_0 - c \int_0^t \cos\theta(t')dt')\ \delta(y - y_0 - c \int_0^t \sin\theta(t')dt')\ \rangle. \quad (6.34)$$

Expressing the 6-functions in terms of the Fourier transforms, we obtain

$$P(x,y,t;x_0,y_0,0) = \left(\frac{1}{2\pi}\right)^2 \int_{-\infty}^{\infty} d\omega_x \int_{-\infty}^{\infty} d\omega_y \; e^{i[\omega_x(x-x_0)+\omega_y(y-y_0)]} \\ \left(\exp\left[-ic\int_0^t [\omega_x \cos\theta(t') + \omega_y \sin\theta(t')]dt'\right] \right). \qquad (6.35)$$

This statistical average can be evaluated by a cumulant expansion [155], and since we have an expression for moments of all orders, we can in principle evaluate the cumulant expansion to any desired order. Truncation of the cumulant series after the second term yields the result of Ref.[153] for the probability distribution:

$$\begin{aligned} P(x,y,t;x_0,y_0,0) &= \frac{1}{2\pi det(M)} \exp\left\{-\frac{M_{ij}^{-1}}{2}(\vec{r}-\vec{r_0}-\vec{a})_i(\vec{r}-\vec{r_0}-\vec{a})_j\right\} \\ \vec{a} &= \frac{2c}{\Gamma}(1-e^{-\Gamma t/2})(\cos\theta_0, \sin\theta_0) \\ M_{ij} &= \langle\, (\vec{r}-\vec{r_0})_i(\vec{r}-\vec{r_0})_j \,\rangle - \langle\, (\vec{r}-\vec{r_0})_i \,\rangle\langle\, (\vec{r}-\vec{r_0})_j \,\rangle \end{aligned} \qquad (6.36)$$

The distribution is Gaussian in this approximation and similiar to the distribution for the traditional Ornstein Uhlenbeck process given in the previous Chapter. Thus it does not exactly preserve the light cone and would appear to constrain the speed only in an average sense. Higher cumulants would be required to describe this feature of fixed speed.

6.3.2 An approximate solution for strong, isotropic scatterers

An approximate solution which preserves the light cone can be obtained under the assumption that 6 is completely randomized in time t*, so that θ has a uniform distribution over $[0, 2\pi]$. This can be justified in the limit of large force strength (Γ), when the scattering events change the momentum by a large amount. Now the time can be discretized on this time-scale and the probability distribution can be written

$$P(x,t;x_0,0) = \frac{1}{2\pi}\int_{-\infty}^{\infty} d\omega \; e^{i\omega(x-x_0)} \left(\exp[-i\omega c \sum_{j=1}^{n} \cos\theta_j t^*] \right), \qquad (6.37)$$

where we have used that at t = 0, the angle 6 was uniformly distributed and have assumed y-invariance, or a line source. To evaluate the average, we will use the fact that in this approximation, each θ_j is independent of all others, giving

$$\left(\exp[-i\omega c \sum^{n} \cos\theta_j t^*] \right) = [J_0(\omega c t^*)]^n , \qquad (6.38)$$

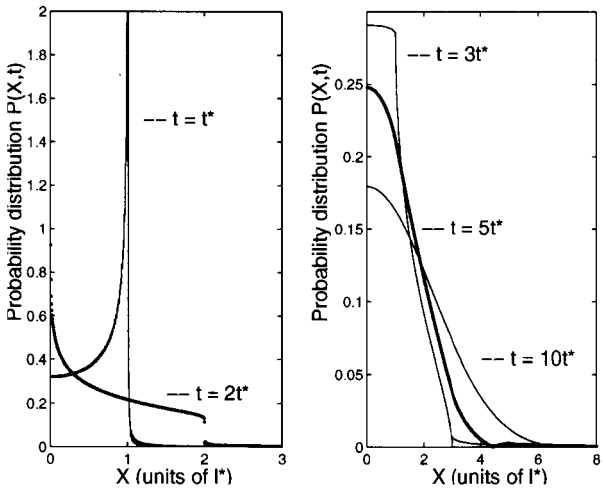

Figure 6.2: The marginal probability distributions $P(x,\mathrm{t};x_0,0)$ predicted by the approximate solution given by equation(28) at different times indicated in the figure. There is a clear cut-off at the light front and initially the probability accumulates at the light front (for t = t*).

where J_0 is the Bessel function of order zero. Using n $= t/t^*$, we have

$$P(x,t;x_0,0) = \frac{1}{2\pi}\int_{-\infty}^{\infty} d\omega e^{i\omega(x-x_0)}\left[J_0(\omega ct^*)\right]^{t/t^*} \tag{6.39}$$

Using the fact that the Fourier transform of $J_0(\omega ct^*)$ is zero for $|x - x_0| >$ ct* and the fact that $P(x,\mathrm{t},x_0,0)$ is an n^{th} convolution of $J_0(\omega ct^*)$, it is seen that $P(x,\mathrm{t},x_0,0)$ is zero for $|x - x_0| > nct^* =$ ct. Thus the light cone is preserved. In Fig. (6.2), we plot the $P(x,\mathrm{t},x_0,0)$ obtained by numerical evaluation for different times. It is seen that for t = t*,the probability is accumulated at the light front, and all the curves show a cut-off at $|x - x_0| =$ ct. At long times, using the Laplace approximation, we have (for large n):

$$\begin{aligned}\left[J_0(\omega ct^*)\right]^n &\simeq \exp\left\{-\frac{c^2t^{*2}\omega^2 n}{4}\right\},\\ P(x,t;x_0,0) &\simeq \left(\frac{1}{\pi c^2 t^* t}\right)^{1/2}\exp\left\{-\frac{(x-x_0)^2}{c^2t^*t}\right\}.\end{aligned} \tag{6.40}$$

Thus, we recover the diffusion limit at long times.

6.3.3 Numerical solutions in the phase space

In this Section, numerical solutions for the differential equation (6.19) (in two dimensions) are presented. The particle is released in the x – y plane at the origin

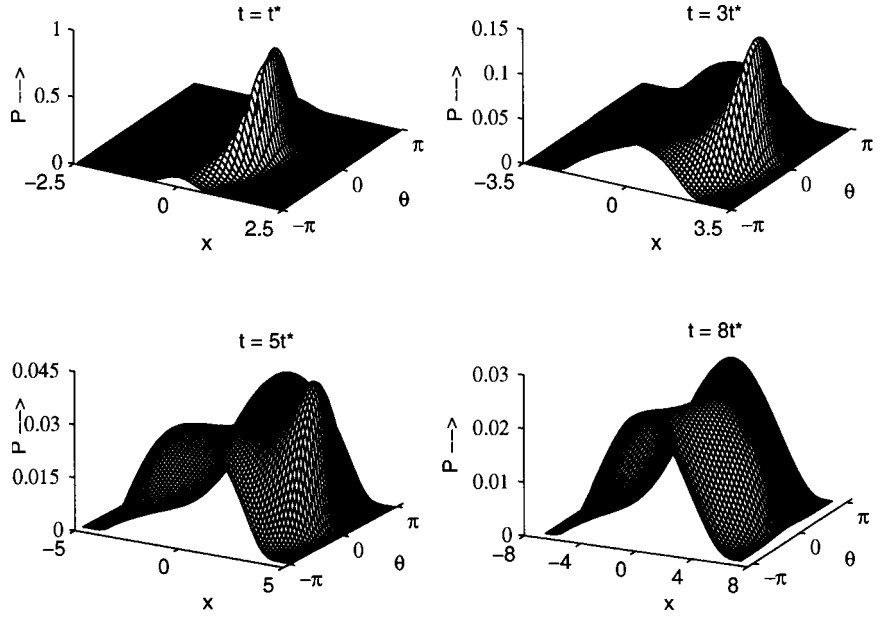

Figure 6.3: The Probability distributions (P) in the phase space of a particle in an infinite medium at different times obtained by numerically propagating equation(17). The particle is released at $X = 0$ along the positive X direction($\theta = 0$) at $t = 0$. The probability distribution is clearly forward peaked and and becomes almost flat along the θ-axis only at times of about $8t^*$.

(generally) along an initial direction θ_0. Here θ is the angle made by the velocity vector with the x-axis. Let us first further simplify by assuming invariance with respect to y, *i.e.*, we have a line source along the y axis. Then the derivative with respect to y drops out and and we have a partial differential equation in three variables. This is essentially a parabolic equation with an advective term. To numerically propagate the probability distribution in time, we use an alternating direction implicit -explicit method [156] for X and θ. A local von Neumann stability analysis [156] shows that this differencing scheme is unconditionally stable. The initial condition is a δ-function at $X = 0, 0 = 0$ which is approximated by a sharp Gaussian for numerical purposes. For numerical stability, we cannot have the Gaussian sharper than a certain amount and in our case the full width at half maximum (FWHM) should be larger than about *8* discretization units. For infinite media, the boundary conditions used were $P(x,t) = 0$ for $|x| > ct$ and periodic boundary conditions on θ.

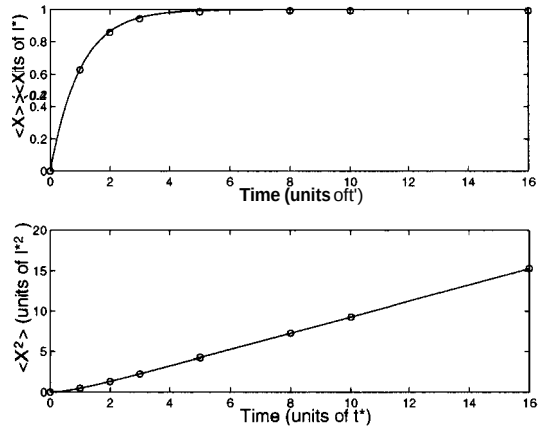

Figure 6.4: The first and second moments of the displacement for the probability distribution of a particle in an infinite medium. The solid lines show the analytical result of equation(20) and equation(22) while the symbol (o) show the result obtained from the numerical solutions.

In Fig. 6.3, we show the probability distributions in an infinite medium with the initial condition, $P(x,\theta,\mathrm{t}=0)=\delta(x)\delta(\theta)$. It is clearly seen that the probability distribution for times upto 5t* is peaked in the forward direction 8 $\sim$ 0 for x $>$ 0, with a tail in the backward direction (8 $\sim \pm\pi$) at x $<$ 0. There is also a clear cut off at $|x|=ct$, which is prominently noticeable for positive x. The small amount of tailing arises from the finite width of the Gaussian by which the 6-function was approximated. One can also note that the probability distribution becomes almost flat along the 8-axis only at times of about eight times the mean free time ($8t^*$). In Fig. 6.4, the first and second moments of the x co-ordinate are shown. The solid lines show the analytical results of equation (6.25 and 6.27) and the symbols(o) represent the results of the numerical solutions. Excellent agreement is found between them. In Fig. 6.5, we show the marginal probability distribution for x *i*.e., $P(x,\mathrm{t};x_0,\theta_0,0)=\int_{-\pi}^{\pi}d\theta P(x,8,\mathrm{t};x_0,\theta_0,0)$. At short times (t $\simeq 3t^*$), there is a clear ballistic peak, separate from the more randomized tail. The probability distribution for these times is also clearly forward-peaked. One can also note that the probability distribution randomizes and becomes almost Gaussian, centred at x $\sim l^*$ only at times t $\geq 8t^*$. As noted above, this is also the time by which the angular coordinate 8 randomizes. This is when the diffusion approximation becomes valid. This can be understood by noting that, by equation(6.7), the time required for $P_t(\theta)$ to attain an angular

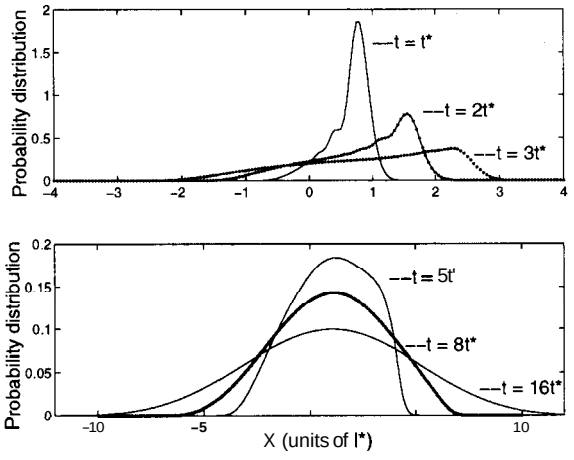

Figure 6.5: The marginal probability distribution $P(x,\mathrm{t};x_0,\theta_0,0)$ $\int_{-\pi}^{\pi} P(x,\theta,\mathrm{t};x_0\theta_0,0)d\theta$ at different times. The marginal probability distribution becomes almost a Gaussian at times of $8t^*$.

width of 2π is T where T is given by $\langle\Delta\theta^2\rangle = (2\pi)^2 \sim 2\Gamma T$. This yields (using $\Gamma/2 = \mathrm{t}^*$) a value of $\mathrm{T} = \pi^2 t^* \simeq 10t^*$ for the randomization time. Thus we now have a clear picture of the reason for this long known experimental fact [20]. This forward peaked behaviour at short times also illustrates the deficiency of the second cumulant approximation where the probability distribution is a Gaussian and symmetric about the first moment. Higher cumulants are clearly required to describe these asymmetric features.

Now let us look at the probability distribution function in the real $(\vec{r})$ space without assuming y-invariance. For this, we solve the Fokker-Planck equation(6.19) in two dimensions, i.e., involving x, y and 8 and integrate over all the directions (8) to get the marginal probability distribution $P(x,\mathrm{y};t)$. This distribution function is plotted in Fig. 6.6 at time $\mathrm{t} = 2t^*$. It is clearly seen that apart from the ballistic peak, the particles begin to spread around in the form of an expanding ring. This is due to the fact that the particles have to diffuse over the velocity circle before their velocity can be reversed. The ring, which has very little probability density in the centre for short times, "fills out" gradually in the middle at longer times, as the diffusion approximation becomes more valid. We can see from here that any Gaussian approximation would be very far from describing the true situation at these times.

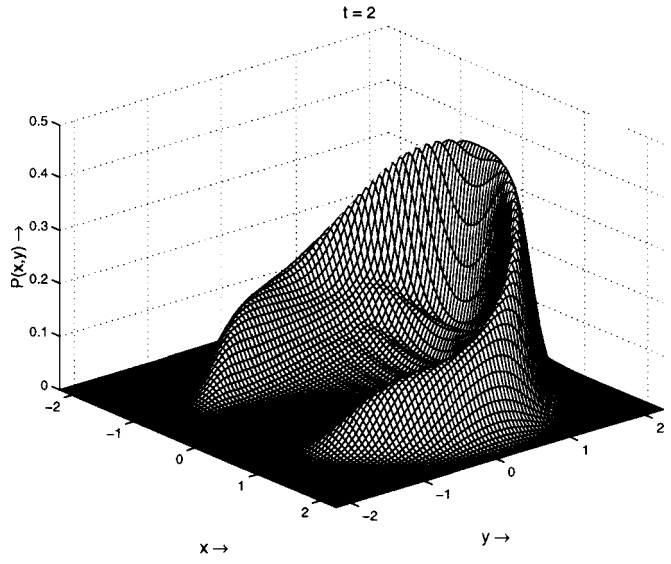

Figure 6.6: The marginal probability distribution function in real space showing a hollow ring -like structure at short times t $= 2t^*$.

6.4 Solutions in bounded media with absorbing boundaries

6.4.1 A semi-infinite medium

For a semi-infinite medium $-\infty <$ x $<$ L with an absorbing boundary at x $=$ L, the appropriate boundary condition is given by $P(L, 0, \mathrm{t}; x_0, \theta_0, 0) = 0$ for $-\pi < 0 < -\pi/2$ and $\pi/2 < 0 < \pi$, corresponding to no flux entering the medium from free space. Also, we can write the Fokker-Plank equation in the form of a continuity equation.

$$\frac{\partial P}{\partial t} + \nabla \cdot \vec{j} = 0 \tag{6.41}$$
$$\nabla = \hat{e}_x \frac{\partial}{\partial x} + \hat{e}_\theta \frac{\partial}{\partial \theta}$$
$$\vec{j} = \hat{e}_x \cos\theta P + \hat{e}_\theta \frac{\Gamma}{2} \frac{\partial P}{\partial \theta}$$

Since $\Gamma = 0$ outside the medium, we can conclude that the current density $\vec{j}$ in the real (x) space is conserved across the boundary in the forward direction $(-\pi/2 < 6 < \pi/2)$ while the current density in the velocity (θ) space is not conserved. This explains why the output flux at the boundary is proportional to the value of the probability distribution function at the boundary itself (rather than the space derivative of the probability distribution $(\partial P/\partial x)$ given by Fick's law) as observed in experiments

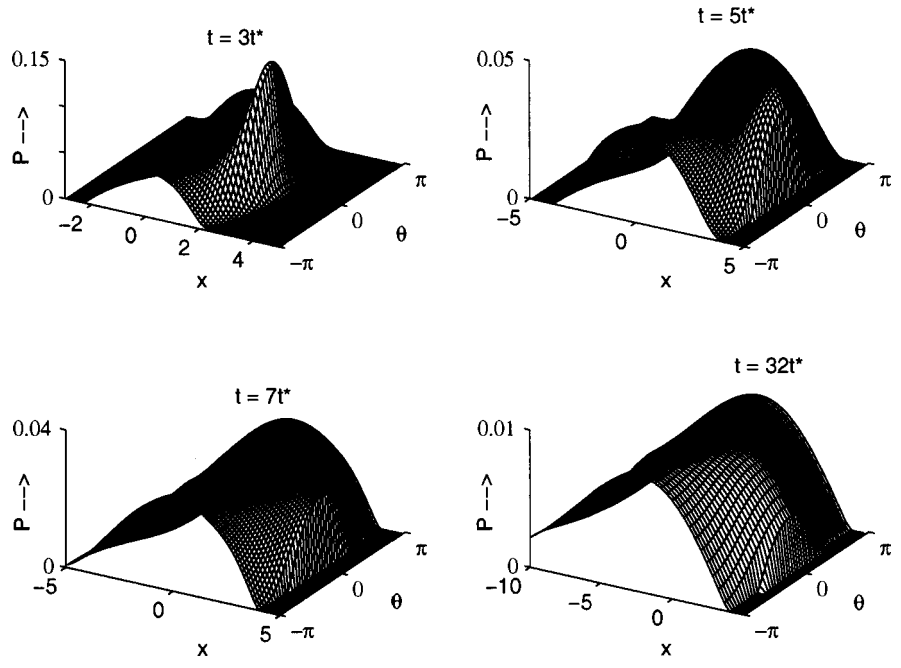

Figure 6.7: The Probability distributions (P) in the phase space of a particle in a semi-infinite medium at different times. The particle is released at x = 0 along the positive x direction($\theta = 0$) at t = 0. The absorbing boundary is located at $4l^*$. The probability distribution is zero in the range $-\pi < 8 < -\pi/2$ and $\pi/2 < 8 < \pi$ at the boundary implying there is no incoming flux into the medium.

[157].

The probability distribution functions for a semi-infinite medium are shown in Fig. 6.7. Here the particle is released at the origin inside the random medium and the initial direction is towards the boundary (in this case at x = $4l^*$). For times lesser than $4t^*$, there is no difference in the probability distribution from the case of the infinite medium. This is because the wave front has not propagated upto the boundary and the effect of the boundary is not felt. This is to be contrasted with the diffusion approximation where the effect of the boundary is felt everywhere simultaneously and causality is violated. At long times the probability distributions attain a typical shape with a long tail at negative x within the medium and a sharp cut-off at the boundary. In Fig. 6.8, we show the marginal probability distribution for x *i.e.*, $P(x,t;x_0,\theta_0,0) = \int_{-\pi}^{\pi} d\theta P(x,\theta,t;x_0,\theta_0,0)$. The value of $P(x,t;x_0,\theta_0,0)$ is finite at the boundary and zero outside. As seen in Fig. 6.8b, if the points near

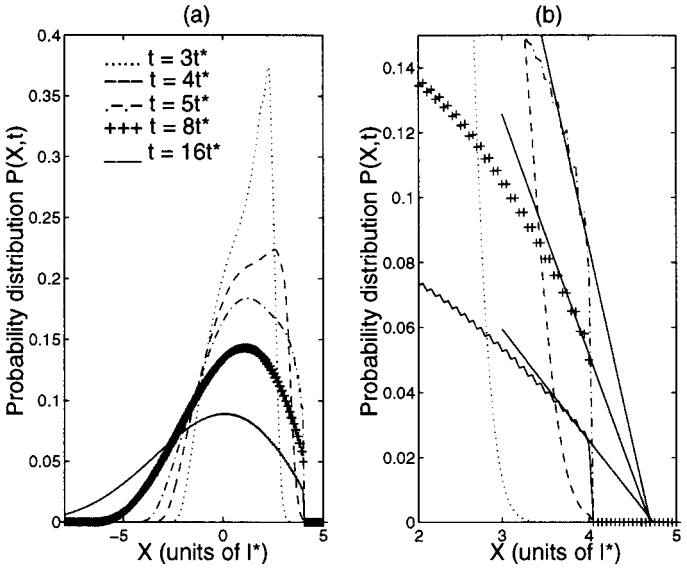

Figure 6.8: The marginal probability distributions in a semi-infinite medium with an absorbing boundary at x $= 4l^*$. The plot on the right shows an expanded view of the distributions near the boundary. The solid straight lines are the linear extrapolations of the behaviour near the boundary. All of them are seen to cross the x-axis roughly at $0.7l^*$ outside the boundary.

the boundary are linearly extrapolated outside the boundary, they all roughly cross the x-axis at about $0.7l^*$, which is the value of the extrapolation length used in the diffusion approximation [146]. In Fig. 6.9, the surviving probability inside the medium $P_s = \int \mathrm{dx} \int d\theta P(x,\theta,t;x_0,\theta_0,0)$ is plotted with time. For long times, this quantity should scale as $t^{-\vartheta}$ where ϑ is the persistence exponent for this process [22]. We have performed these calculations for several source-boundary distances and obtained a value of 0.435 ± 0.005 as the persistence exponent for this process in two dimensions.

6.4.2 A finite slab

Now, we present solutions for a finite slab with absorbing boundaries at x $= \pm L$. The particle is released from the origin at $t = 0$ along the positive x direction at x $= -$L. Fig. 6.10a shows the first and second moments of the probability with time in a thin slab of thickness $2l^*$. The first and second moments initially increase as in an unbounded medium until the photon-front hits the boundary and dip before increasing again and saturating at an almost constant value. The dips occur

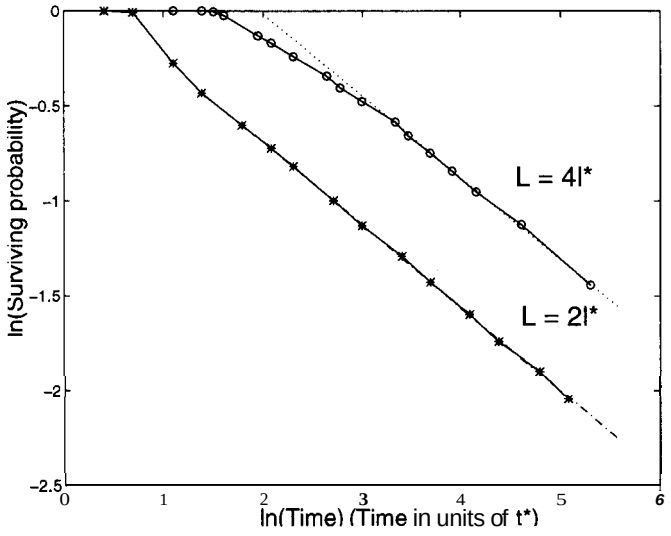

Figure 6.9: The surviving probability of the particle inside the semi-infinite medium for an absorbing boundary at $4l^*(\circ)$ and $2l^*(*)$. The persistence exponent θ is obtained from the long time behaviour of the survival probability. The lines $(\cdots)$ and $(- \; . \; -)$ show the linear fits and give a persistence exponent of 0.4309 and 0.4364 respectively.

because just after the ballistic and near ballistic components exit the slab, only the photons which are effectively moving in the opposite directions are left behind. This is a manifestation of the fact that the cloud expands out in a hollow ring, as seen before. In fact, the first moment is seen to become negative, implying that the net transport is in the backward direction for some time. The dip in the second moment implies that the photon cloud is effectively expanding at a slower rate. This would cause a lowered 'effective diffusion coefficient' to be measured in a pulse transmission measurement [17]. This reinforces the conclusions reached in Ref.[151] based on Monte-carlo simulations. Fig.6.10b shows the survival probability for the case of a finite slab. This decays considerably faster than the in case of the semi-infinite slab, though at early times ($t \sim t^*$) the decay rates are comparable. The initial rates of decay are comparable because of the forward peaked nature of the probability distribution at early times, when the effect of the boundary at the back is hardly felt. This is to be compared with the mirror-image solution in the diffusion approximation, where equal weightage is given to both boundaries at all times.

Now, let us look at the temporal evolution of the spatial intensity profiles of the

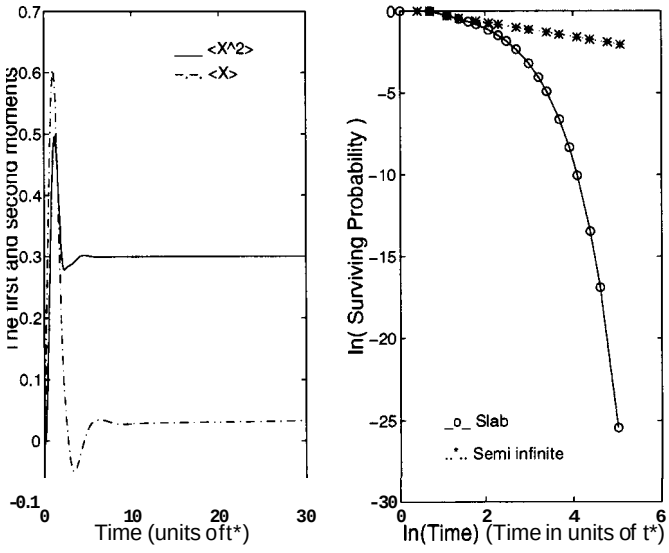

Figure 6.10: The first and second moments of the displacement of a particle in a finite slab of thickness 21* (left plot). The right plot shows the survival probability in a semi-infinite medium and a finite slab. The distance between the point where the particle is released and the boundary is same in both case. $(2l^*)$.

transmitted light for the incident point source. This is equivalent to studying the dynamics of the point spread function in time. We take a thin slab with absorbing boundaries. and propagate the initial distribution, i.e., the photon is incident along the positive x-axis at x $= -L$ and $t = 0$. The slab is assumed to be of infinite tranverse extent as before, but, no y-invariance is assumed. Now, we look at the transmitted near-field probability distribution along the y-axis. We plot these profiles in Fig. 6.11. At $t = L/c$, we see the ballistic peak emerging out of the slab. For slightly larger times and a reasonably thin slab, the transmitted profiles consist of two peaks with a dip in the centre at y $= 0$. These peaks move apart in time, while the centre slowly 'fills out' in time. This means that for a 3-D system, the transmitted near-field intensity appears as a ring for intermediate times after the exit of the ballistic pulse. This ring grows in size as well as diffuses out, eventually giving the distribution predicted by the diffusion approximation. Again, these features result from the persistence in the velocity space of the random photon walks. These features, however, smoothen out for thick slabs (L $> 4l^*$) as the distribution would have already randomized in the angular coordinate to quite an extent by the time the photons exit.

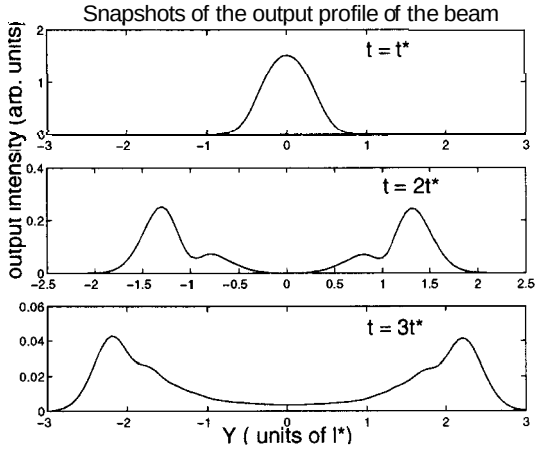

Figure 6.11: The near field spatial profiles of the transmitted light through a thin slab at different times

6.5 Random Amplifying Media

As discussed in Section-1.5.1, a random medium with amplification can turn into a laser. We will now apply this model of photon diffusion with constant speed to the case of an amplifying stochastic medium. The effect of medium gain can be incorporated straight forwardly by noting that in our treatment, the time of exit from the slab directly translates into path-length traversed within the medium because speed is kept absolutely fixed. In the presence of amplification in the medium therefore, the net gain is directly proportional to the time. Thus the output flux at the boundary in a given direction is simply $P(L,\theta,\mathrm{t})\cos\theta\exp(\alpha t)$, where $\mathbf{a}$ is the gain coefficient in the medium. It is thus simple to obtain a picture of amplified emission from such a medium. In Fig. 6.12, we show the total light emitted by slab (from both sides) with boundaries at $\mathrm{x} = \pm 2l^*$ for several amplification factors. The photon is released from the origin in the positive x-direction. We see that output increases with increasing gain factor. However, upto a critical gain factor, the output in time goes through a (ballistic) peak and then reduces in time. Beyond the critical gain coefficient $(\mathbf{a} = 0.19)$, the output increases exponentially in time. This is because the random amplifying medium has now crossed the critical threshold and has now become a random laser. For large times, the output increases exponentially because

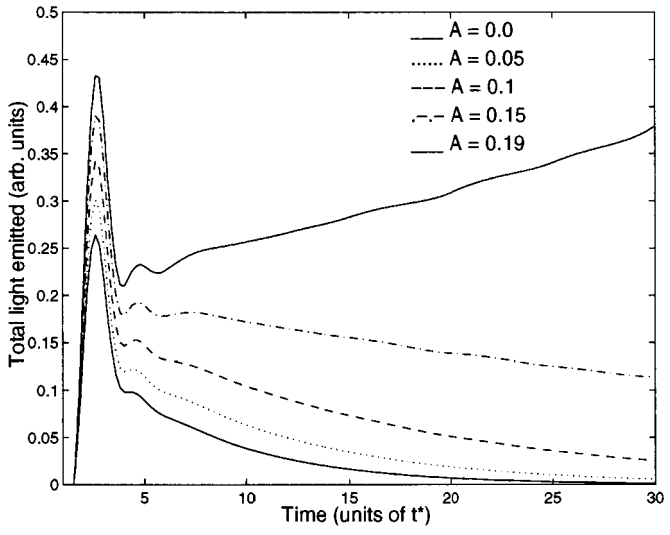

Figure 6.12: Total light emitted (from both sides) by a disordered slab with amplification for different values of the gain coefficient A in the medium. The output increases exponentially at long times.

of the presence of a exponential gain in the medium with no saturation. It is seen that the ballistic part is only slightly amplified while the output in the tail regions are increased considerably. To obtain a more realistic picture of lasing in random media [16, 54], however, one would have to consider the lasing level population depletion and saturation effects.

6.6 Conclusions

In this Chapter, we have developed a model for photon migration which dynamically preserves the local constraint of fixed speed , i.e., the 'strong' constraint for fixed speed. The propagation of light in a scattering medium is described as the motion of a special kind of a Brownian particle on which the fluctuating forces act only perpendicular to its velocity. This enforces strictly and dynamically the constraint of constant speed of the photon in the medium. A Fokker-Planck equation is derived for the probability distribution in the phase space assuming the transverse fluctuating force to be a white-noise. Analytic expressions for the moments of the displacement (x^n) along with an approximate expression for the marginal probability distribution function $P(x,t)$ are obtained. Exact numerical solutions for the phase space probability distribution for infinite (unbounded) media and media with absorbing boundaries

(semi-infinite media and finite slabs) have been presented. The results show that the velocity distribution randomizes in a time of about eight times the mean free time ($8t^*$) only after which the diffusion approximation becomes valid. This factor of eight is a well known experimental fact. Absorption or gain is very easily implemented in this model because time directly translates to the path length in the medium, as the speed has been kept locally fixed.

We note that the problem of diffusion of a particle moving with constant speed is of interest in several areas. Its application to the motion of an electron in a random magnetic field is obvious [158]. Another application of this model is to the theoretical description of semi-flexible chains in polymer physics. These stiff filaments are represented by an inextensible curve $\vec{r}(s)$, where s is the arc-length, $|d\vec{r}/ds|$ being constant [159]. This problem can be mapped exactly into the current problem of photon diffusion at constant speed.

Finally, we point out that though this treatment is a radiometric calculation, it is not necessarily inaccurate as a description of wave motion. As has been pointed out in Section 1.3.4, the specific intensity describing the energy transport is related to the mutual coherence function describing the wave motion and a surprising amount of wave characterestics can be incorporated. In this problem, we have incorporated one of the wave characterestics, *viz*, the constant speed (group velocity) of the wave in between the scattering events. We worked in the limit $ka \gg 1$ where a is the inter-scatterer distance and k is the wavevector. Even when the $ka \sim 1$, it has been experimentally found that [160] that the primary effect appears to be a renormalization of the group velocity of light. In this picture, the effects of dispersion can also be incorporated to a first approximation by making the speed $c(k)$ a function of the wavevector and taking an appropriate distribution of speeds to describe the wavepacket.

Chapter 7

Diffusive transport with inertia: the generalization of the Telegrapher process to higher dimensions and a model phase space

7.1 Introduction

The diffusion equation admirably describes the the incoherent transport of the energy density of light at a gross-level but fails, however, to describe the transport accurately at short length scales ($l < 8l^*$ where l^* is the transport mean free path) and at short time scales ($t < 8t^*$, where $t^* = l^*/c$ is the transport mean free time) [20]. Among the many models proposed to deal with the intermediate range of length- and time-scales between the ballistic motion and diffusive transport, the attempts to generalize the Telegrapher equation are important. The Telegrapher equation is exact in one dimension and describes the diffusion of a particle whose speed is fixed, i.e., the velocity can take on only two values $\pm c$ [161]. The Telegrapher equation, i.e,

$$\frac{\partial^2 P}{\partial t^2} + \Gamma \frac{\partial P}{\partial t} - c^2 \frac{\partial^2 P}{\partial x^2} = 0, \tag{7.1}$$

where P is the probability distribution function and $\Gamma/2$ is the mean scattering rate, is a combination of the wave equation describing the inertial aspect and of the diffusion equation describing the stochastic aspect. This equation has found wide application in many fields [162] and was first considered by J.C. Maxwell [163, 164], more than a century ago in his attempt to describe heat conduction from basic kinetic theory. It also has been shown to describe the 'second sound' in liquid Helium II.

Following a suggestion of Ishimaru [165], a generalization of the Telegrapher equation to higher dimensions in a heuristic manner was attempted [166] by simply replacing $\partial^2 P/\partial x^2$ in Eqn.(7.1) by $\mathrm{V}^2\mathrm{P}$, to describe photon migration at short length scales, by including some ballistic aspects. This ad-hoc generalization appeared to be quite successful to describing photon migration as it preserved causality and did much better than the diffusion approximation to describe photon transport in absorbing media [166, 167]. This was also extended to studies of Diffusing Wave Spectroscopy in thin samples [168]. It was, however, shown by comparing it with Monte-Carlo simulations that this generalization furnished no better an approximation than the diffusion approximation in higher dimensions [169]. The in-principle weakness of this 'ad-hoc' approach was demonstrated by the fact that the photon probability density evolving under this equation becomes negative in two dimensions for the simplest case of an unbounded (infinite) medium at short times ($t \sim t^*$) when the ballistic aspects of transport are most important. In fact, the negativity of the solution to this equation is a generic property in even-dimensional spaces [169, 146].

In this Chapter, we reconsider the problem of diffusion of photons at constant speed and present a generalization of the Telegrapher process to higher dimensional turbid media ($d > 1$), where the photon can move along 2^d directions along the diagonals of a d-dimensional hypercube. We derive the equation for the probability density function using the "formulae of differentiation" of Shapiro and Loginov [101], by considering a correlated random walk at constant speed. We show that a partial differential equation of order 2^d results for the probability distribution function in d-dimensions. Our model is an advancement over the earlier models of Boguñá *et al.* [170, 171], where the photon could only move along the 2d directions along the axes, and results in a true diffusion at constant speed in the limit of large dimensions. Our work brings out certain features that were not recognized in earlier work. Light in the stochastic medium is considered to be a particle on which the medium exerts fluctuating forces. Each scattering event only changes the direction of the photon without affecting the speed of propagation.

7.2 The Telegrapher process in one dimension

Let us first consider the dynamics of a particle executing a random walk in one dimension while moving with constant speed c. This would describe the motion of light in a disordered fibre, or of electrons on the Fermi points in a one-dimensional disordered wire, if we neglect the wave nature and the consequent Anderson localization (Strictly speaking, this description would not hold for 1-D where all the quantum states are localized states. For sample lengths much smaller than the localization length, however, the transport is almost diffusive). The velocity $v(t)$ of the particle is a random function of time such that it can take only two values $\pm$c, i.e., a Dichotomic Markov process. If $\Gamma/2$ be the transition probability per unit time between these two values of the velocity (( ) indicate averaging over the disorder),

$$\langle v(t) \rangle = 0, \tag{7.2}$$

$$\langle v(t)v(t') \rangle = c^2 \exp(-\Gamma|t-t'|), \tag{7.3}$$

i.e. the velocity is exponentially correlated in time. We note that the stochastic Langevin equation for the displacement x $= v(t)$ gives:

$$\langle x \rangle = 0, \tag{7.4}$$

$$\langle x^2 \rangle = \frac{2c^2}{\Gamma}(t - \frac{1-e^{-\Gamma t}}{\Gamma}), \tag{7.5}$$

i.e., the behaviour at long times (t $\rightarrow \infty$) or very large scattering strengths (large Γ) is diffusive ($\langle x^2 \rangle \sim$ t) and at short times (t $\rightarrow 0$), the behaviour is ballistic ($\langle x^2 \rangle \sim t^2$).

Now we will derive the equation for the probability distribution function. Let $\Pi(x;t)$ be the phase space density of points in the x-t phase space. Now, Π satisfies the Stochastic Liouville equation :

$$\frac{\partial \Pi}{\partial t} + \frac{\partial}{\partial x}(\dot{x}\Pi) = 0. \tag{7.6}$$

Averaging over all the realizations of the random function $v(t)$, by the van Kampen lemma [98], the probability distribution $P(x;t) = \langle \Pi(x;t) \rangle$. We also define W(x;t) $= \langle v(t)\Pi(x;t) \rangle$ and obtain,

$$\frac{\partial P}{\hat{a}\, t} + \frac{\partial W}{\partial x} = 0. \tag{7.7}$$

Now using the "formulae of differentiation" of Shapiro and Loginov [101], for a Dichotomic Markov process,

$$\frac{\partial W}{\partial t} = -\Gamma W - c^2 \frac{\partial P}{\partial x}. \tag{7.8}$$

Eliminating W from the above equations, we obtain

$$\frac{\partial^2 P}{\partial t^2} + \Gamma \frac{\partial P}{\partial t} = c^2 \frac{\partial^2 P}{\partial x^2}, \tag{7.9}$$

i.e. the Telegrapher equation for the probability distribution function **P.** This is an exact description of the motion of a particle with constant speed in 1-D.

The solutions to Equation.(7.9) are well known and, in an infinite medium given by [161, 166]

$$P(x,t;x=0,t=0) = \left(\frac{\Gamma}{2c}\right) e^{-\Gamma t/2}[I_0(y) + 2\Gamma t \frac{I_1(y)}{y}]\ \theta(ct-|x|), \tag{7.10}$$

where y $= (\Gamma/2c)\sqrt{c^2t^2 - x^2}$, I_0 and I_1 are the modified Bessel functions of order zero and one respectively, and θ is the Heaviside step function. Note that the solution is zero for $|x| >$ ct and thus causality is preserved. The solution indicates that the particles spread out symmetrically from the origin, half of them to the left and the other half to the right, with a front velocity of c beyond which there are no more particles and heap up at the 'light fronts' where there are $N/2\exp(-\Gamma t/2)$ particles (if there are N particles altogether).

Another approach to obtain the above is to consider that the photon density is made of two separate partial flux components: one consisting of particles moving upstream and another downstream. The scattering couples these two partial fluxes:

$$\frac{\partial I_\uparrow}{\partial t} = c\frac{\partial I_\uparrow}{\partial x} - \sigma_a I_\uparrow - \sigma_s p_b I_\uparrow + \sigma_s p_b I_\downarrow, \tag{7.11}$$

$$\frac{\partial I_\downarrow}{\partial t} = -c\frac{\partial I_\uparrow}{\partial x} - \sigma_a I_\downarrow - \sigma_s p_b I_\downarrow + \sigma_s p_b I_\uparrow, \tag{7.12}$$

where $a,$ and $a,$ are the scattering and absorption coefficients and p_b is the backscattering probability. We immediately note that our $\mathbf{P} = I_\uparrow + I_\downarrow$, the photon density and W $= I_\uparrow - I_\downarrow$ (the equivalent of the osmotic density of Nelson[81]). We also note that heuristic attempts have been made to adapt the above "two-stream" theory to describe transport in higher dimensions by, i) modifying the values of the coefficients to phenomenologically fit experiments, resulting in the Kubelka-Munk two-flux equations[11], and ii) by introducing more number of streams[11].

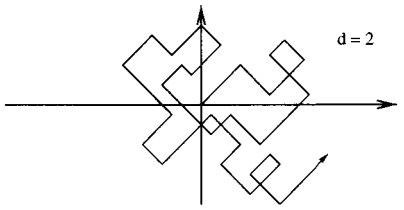

Figure 7.1: One realization of the possible real space trajectories for the generalized Telegrapher process in two dimensions.

7.3 Generalization of the Telegrapher process to higher dimensions

Now, we seek a generalization of the Telegrapher process process to higher dimensions. The simplest way of doing this is to make every orthogonal component a dichotomic Markov process which take the values $\pm$c. Thus, in d dimensions, the particle is seen to move along the diagonals of the d dimensional hypercube with a speed $\sqrt{d}c$. Here the real space is continuous, while the the velocity space is discrete and can take only 2^d discrete values in d dimensions. This is the model phase space that we consider the photon to execute a random walk in. In Fig. 7.1, we show a possible trajectory in the real space for d = **2.**

7.3.1 The equations for the generalized Telegrapher process

In two dimensions, we will consider both the x and y components of the velocity of the particle to be independent dichotomic Markov processes,

$$v_x(t) = c\chi_1(t), \tag{7.13}$$

$$v_y(T) = c\chi_2(t), \tag{7.14}$$

$$\langle \chi_i(t) \rangle = 0, \tag{7.15}$$

$$\langle \chi_i(t)\chi_j(t') \rangle = \delta_{ij} \exp(-\Gamma|t - t'|), \tag{7.16}$$

where $\chi_i(t)$ are unimodular processes. The particle is thus seen to move along the four directions $(\pm\hat{i}, \pm\hat{j})$ with a constant speed $\sqrt{2}c$. Now using the stochastic Louiville equation, We define the averages $P(x, y; \mathrm{t}) = \langle \Pi(x, y; \mathrm{t}) \rangle$, $W_x = \langle v_x(t)\Pi(x, y; \mathrm{t}) \rangle$, $W_y = \langle v_y(t)\Pi(x, y; \mathrm{t}) \rangle$ and $W_{xy} = \langle v_x(t)v_y(t)\Pi(x, \mathrm{y}; \mathrm{t}) \rangle$. We also note that the "formula of differentiation" of Shapiro and Loginov can be generalized to n-independent

dichotomic Markov processes (see Appendix-C) as

$$\begin{aligned}\frac{d}{dt} \quad & \langle \quad v_1 v_2 \cdots v_n \Pi[v_1, v_2, \cdots v_n] \rangle_{v_1, v_2, \cdots, v_n} = \\ = \quad & -(\Gamma_1 + \Gamma_2 + \cdots + \Gamma_n) \langle v_1 v_2 \cdots v_n \Pi[v_1, v_2, \cdots, v_n] \rangle_{v_1, v_2, \cdots v_n} \\ + \quad & \langle v_1 v_2 \cdots v_n \frac{d\Pi[v_1, v_2, \cdots v_n]}{dt} \rangle_{v_1, v_2, \cdots, v_n}, \end{aligned} \tag{7.17}$$

where $v_i(t)$ are independent dichotomic Markov processes, Γ_i are the respective transition rates and Π is a functional of v_1, v_2, $\cdots$, v_n. Using the above, we obtain the following closed set of equations :

$$\frac{\partial P}{\partial t} + \frac{\partial W_x}{\partial x} + \frac{\partial W_y}{\partial y} = 0, \tag{7.18}$$

$$\frac{\partial W_x}{\partial t} + \Gamma W_x = -c^2 \frac{\partial P}{\partial x} - \frac{\partial W_{xy}}{\partial y}, \tag{7.19}$$

$$\frac{\partial W_y}{\partial t} + \Gamma W_y = -c^2 \frac{\partial P}{\partial y} - \frac{\partial W_{xy}}{\partial x} \tag{7.20}$$

$$\frac{\partial W_{xy}}{\partial t} + 2\Gamma W_{xy} = -c^2 \left[\frac{\partial W_y}{\partial x} + \frac{\partial W_x}{\partial y} \right]. \tag{7.21}$$

Eliminating W_x, W_y, W_{xy} from the above set of equations, we obtain for the probability distribution function $P(x, y; t)$:

$$\frac{\partial}{\partial t}\left(\frac{\partial}{\partial t} + 2\Gamma\right)\left(\frac{\partial}{\partial t} + \Gamma\right)^2 P - 2c^2 \left(\frac{\partial}{\partial t} + \Gamma\right)^2 \nabla^2 P + c^4 \left(\frac{\partial^2}{\partial x^2} - \frac{\partial^2}{\partial y^2}\right) P = 0 \ . \tag{7.22}$$

By performing a $\pi/4$ rotation of the space axes and rescaling the speed to c, this equation is seen to be the same as the one derived by Boğuna et al.[170] by a different approach. Unlike the "ad-hoc Generalized Telegrapher equation" of Durian and Rudnick [166], this partial differential equation is of fourth order involving all space and time derivatives.

Similiarly, in three dimensions, we consider the x, y and z components to the velocity to be independent dichotomic Markov processes. Again, following the above procedure, we obtain the closed set of eight equations :

$$\frac{\partial P}{\partial t} + \frac{\partial W_x}{\partial x} + \frac{\partial W_y}{\partial y} + \frac{\partial W_z}{\partial z} = 0 \tag{7.23}$$

$$\frac{\partial W_x}{\partial t} + \Gamma W_x = -c^2 \frac{\partial P}{\partial x} - \frac{\partial W_{xy}}{\partial y} - \frac{\partial W_{zx}}{\partial z} \tag{7.24}$$

$$\frac{\partial W_y}{\partial t} + \Gamma W_y = -c^2 \frac{\partial P}{\partial y} - \frac{\partial W_{xy}}{\partial x} - \frac{\partial W_{yz}}{\partial z} \tag{7.25}$$

$$\frac{\partial W_z}{\partial t} + \Gamma W_y = -c^2 \frac{\partial P}{\partial z} - \frac{\partial W_{zx}}{\partial x} - \frac{\partial W_{yz}}{\partial y} \tag{7.26}$$

$$\frac{\partial W_{xy}}{\partial t} + 2\Gamma W_{xy} = -c^2\left[\frac{\partial W_y}{\partial x} + \frac{\partial W_x}{\partial y}\right] - \frac{\partial W_{xyz}}{\partial z} \quad (7.27)$$

$$\frac{\partial W_{yz}}{\partial t} + 2\Gamma W_{yz} = -c^2\left[\frac{\partial W_y}{\partial z} + \frac{\partial W_z}{\partial y}\right] - \frac{\partial W_{xyz}}{\partial x} \quad (7.28)$$

$$\frac{\partial W_{zx}}{\partial t} + 2\Gamma W_{zx} = -c^2\left[\frac{\partial W_z}{\partial x} + \frac{\partial W_x}{\partial z}\right] - \frac{\partial W_{xyz}}{\partial y} \quad (7.29)$$

$$\frac{\partial W_{xyz}}{\partial t} + 3\Gamma W_{xyz} = -c^2\left[\frac{\partial W_{yz}}{\partial x} + \frac{\partial W_{zx}}{\partial y} + \frac{\partial W_{xy}}{\partial z}\right] \quad (7.30)$$

It is possible to obtain a cumbersome-looking partial differential equation for P(x,y,z;t) alone, similiar to Equation(7.22) by eliminating the other functions from the above coupled set of differential equations. However, no extra information results and it will not be presented here.

The partial differential equation for $P(\vec{r};t)$ alone, in general, will be of order 2^d (there are 2^d independent first order coupled differential equations for d dimensions). The set of coupled first order differential equations(7.23) offer a very convenient factorization of the 2^d dimensional equation satisfied by $P(\vec{r};t)$ and are a more convenient starting point for numerical calculations of the solutions. We note that the above equations are linear with constant coefficients and can easily be solved by taking Laplace transforms with respect to time and space variables. Inverting the solutions obtained back to the real space-time, however, is non-trivial and only a few characteristic quantities such as the moments of the residence times have been calculated [171] for a similiar model.

7.3.2 Absorbing boundary conditions

For the above system of equations, absorbing boundary conditions can be easily and rigorously applied for this set of equations. For an absorbing boundary at x = 0, with the stochastic medium occupying the negative semi-infinite half-space, the appropriate boundary conditions corresponding to no incoming flux are

$$W_x(x=0,y,z;t) = cP(x=0,y,z;t), \quad (7.31)$$

$$W_{xy}(x=0,y,z;t) = cW_y(x=0,y,z;t), \quad (7.32)$$

$$W_{zx}(x=0,y,z;t) = W_z(x=0,y,z;t), \quad (7.33)$$

$$W_{xyz}(x=0,y,z;t) = cW_{yz}(x=0,y,z;t), \quad (7.34)$$

and free boundary conditions on the other functions $\mathbf{P}$, W_y, W_z, W_{yz}. These conditions are equivalent to the integral boundary condition $\partial/\partial t \int_{-\infty}^{x=0} P(x, \mathrm{y}, z; t)dx = cP(x = 0, \mathrm{y}, z; \mathrm{t})$ on $P(x, \mathrm{y}, z; \mathrm{t})$ alone.

7.3.3 Projected motion along any axis and angular non-symmetry of the model

In higher dimensions (d $>$ 1), the *ad-hoc* generalized Telegrapher equation *viz.* $\frac{\partial^2 P}{\partial t^2} + \Gamma\frac{\partial P}{\partial t} - c^2\nabla^2 P = 0$ is indeed obtained only if higher order velocity correlations are neglected, *i.e.*, terms such as $W_{xy} = \langle v_x \Pi \rangle$, W_{xyz} etc. are set to zero. This is not correct especially at short times, when we expect the velocity components to be correlated to a quite some extent. However, it is easily seen that the marginal probability distribution for the projected motion along one of the axis $p(x_1; \mathrm{t}) = \int P(x_1, x_2, \cdots, x_d)dx_1\ dx_2\ \cdots\ dx_d$ satisfies the Telegrapher equation $\frac{\partial^2 p}{\partial t^2} + \Gamma\frac{\partial p}{\partial t} - c^2\frac{\partial^2 p}{\partial x^2} = 0$. The partial differential equation for $P(\vec{r}; t)$ alone, in general, will be of order 2^d (there are 2^d independent first order coupled differential equations for d dimensions) corresponding to 2^d directions.

There are some subtle differences between our model and that of Boguñá et al [170]. First of all, the number of allowed directions for the photon motion is greater in our model (2^d) than theirs ($2d$). The reason is that, they consider that the motion of the particle to be along the axes, while in our case, the motion is along the diagonals of the d dimensional hypercube. They do not obtain a Telegrapher equation for the marginal probability distribution for the projected motion in general as we do. We always have a Telegrapher process along any one axis. This can be best compared in two dimensions by carrying out a $\pi/4$ rotation of the axes in Eqns.(7.18-21) and then looking at the projected motion along the axes. We obtain the Telegrapher equation $\frac{\partial^2 p}{\partial t^2} + 2\Gamma\frac{\partial p}{\partial t} - c^2\frac{\partial^2 p}{\partial x^2} = 0$, *i.e.*, only the diffusion coefficient is renormalized. This corresponds to the three step Telegrapher process of moving at constant speed to the left or the right with a probability 1/4 and being at rest with a probability 1/2. In higher dimensions (d $>$ 2), the diagonals of the hypercube are not orthogonal and the equation obtained for the projected motion along the diagonals is not a Telegrapher equation in our case.

Thus, it is to noted that in these models without angular symmetry, such a de-

scription of projected motion is non-unique and depends on the direction of the projected motion. It should, however, be pointed out that the angular spacing between these discrete directions, given by the ratio of the total solid angle to the number of directions, in our model is

$$\frac{\text{''(d)}}{2^d} - \frac{1}{2^d}\frac{2\pi^{d/2}}{\Gamma(d/2)\,d} \to \left(\frac{\pi^{1/2}e^{1/2}}{2\ln^{1/2}(d/2)}\right)^d, \tag{7.35}$$

where Γ here is the Gamma function. In the limit of large d, the angular spacing decays almost exponentially to zero. Thus, in the limit of large dimensions, this process indeed describes a genuine diffusion at constant speed.

7.4 Kubo-Anderson like stochastic processes

In passing, we would like to touch upon the possible generalization to more complex stochastic processes, which demonstrates the power of the current approach. It is a simple matter now, to write down the equations for probability distribution function for a Kubo-Anderson like process, given by the sum of n-independent dichotomic Markov processes (in one -dimension), i.e., $v(\mathrm{t}) = v_1(\mathrm{t}) + v_2(\mathrm{t}) + \ldots + v_n(\mathrm{t})$, where $v_i(t)$ can take on the values $\pm c$ and $\langle v_i(t)\rangle = 0$; $\langle v_i(t)v_j(\mathrm{t}')\rangle = c^2\exp(-\Gamma|t-t'|)\delta_{ij}$. The structure of the equations for n = 2 and n = 3 remain the same as Eqn. (7.18-21) and Eqn. (7.24-30) respectively, with only the derivatives $\partial/\partial y$ and $\partial/\partial z$ replaced by $\partial/\partial x$. It is immediately seen that the case of n = 2 corresponds to the 3-step Telegrapher processes described above. The generalization to higher n is obvious. In general, one obtains n + 1 coupled partial differential equations for the sum of n-independent dichotomic Markov processes.

7.5 Conclusions

In conclusion, we have developed a particular 'generalization' of the Telegrapher process to higher dimensional (d > 1) stochastic media which could be potentially useful for studying photon migration in turbid media as it rigourously preserves the photon speed to be constant between the scattering events. In cornparision to the model presented in Chapter 6, where the photon's random walk was modelled as a diffusion on the velocity sphere, we have a model phase space here, where the photon can move only along the 2^d directions of the diagonals of the d dimensional hypercube.

It is admittedly an artificial phase space, but one having an appreciable directional persistence unlike the zero-persistence diffusion theory. However, the model does not have angular symmetry. In 1-D, there are only two directions and hence, the Telegrapher equation is exact. On the other hand, in the limit of very large dimensions, the angular spacing between the directions tends to zero almost exponentially, and again the process is indeed a genuine diffusion-at-a-constant-speed. It has been shown that the equation for the projected motion along any hypercube axis is a 1-D Telegrapher equation, though it is non-invariant under a rotation. Further, the ad-hoc generalized Telegrapher equation in higher dimensions [166, 167] is recovered when higher order correlations are neglected. The power of this approach is demonstrated by deriving the equations for a sum of n-independent Markov processes.